

NAVAL POSTGRADUATE SCHOOL
Monterey, California



19980727 150

THESIS

**AN EXAMINATION OF
BI-ORTHOGONALITY RELATIONSHIPS
IN ELASTIC-FLUID MEDIA**

by

Coley R. Myers, III

June 1998

Thesis Advisor:
Thesis Co-Advisor:

Clyde L. Scandrett
Christopher L. Frenzen

Approved for public release; Distribution is unlimited.

THE QUALITY ASSURED 9

REPORT DOCUMENTATION PAGE			Form Approved OMB No. 0704-0188	
Public reporting burden for this collection of information is estimated to average 1 hour per response, including the time for reviewing instruction, searching existing data sources, gathering and maintaining the data needed, and completing and reviewing the collection of information. Send comments regarding this burden estimate or any other aspect of this collection of information, including suggestions for reducing this burden, to Washington Headquarters Services, Directorate for Information Operations and Reports, 1215 Jefferson Davis Highway, Suite 1204, Arlington, Va 22202-4302, and to the Office of Management and Budget, Paperwork Reduction Project (0704-0188) Washington DC 20503.				
1. AGENCY USE ONLY (Leave blank)		2. REPORT DATE June 1998		3. REPORT TYPE AND DATES COVERED Master's Thesis
4. TITLE AND SUBTITLE AN EXAMINATION OF BIORTHOGONALITY RELATIONSHIPS IN ELASTIC-FLUID MEDIA				5. FUNDING NUMBERS
6. AUTHORS Myers, Coley R., III				
7. PERFORMING ORGANIZATION NAME(S) AND ADDRESS(ES) Naval Postgraduate School Monterey CA 93943-5000				8. PERFORMING ORGANIZATION REPORT NUMBER
9. SPONSORING/MONITORING AGENCY NAME(S) AND ADDRESS(ES)				10. SPONSORING/MONITORING AGENCY REPORT NUMBER
11. SUPPLEMENTARY NOTES The views expressed in this thesis are those of the author and do not reflect the official policy or position of the Department of Defense or the U.S. Government.				
12a. DISTRIBUTION/AVAILABILITY STATEMENT Approved for public release; distribution is unlimited.				12b. DISTRIBUTION CODE
13. ABSTRACT(maximum 200 words) The bi-orthogonality relationships for vertically heterogeneous porous media in contact with various surfaces have been previously established. For the special case in which the porous substance has zero porosity, the relationships reduce to those for elastic media. The bi-orthogonality relationship for a fluid loaded elastic slab will be considered numerically by discretizing the boundary value problems using finite differences. The resulting matrix will be analyzed for the purpose of determining eigenvalues of the complex dispersion relationship of the layered media, as well as discerning the corresponding eigenvectors which are discrete analogies of the propagation/evanescent eigenfunctions of the media.				
14. SUBJECT TERMS Acoustics, Biorthogonality, Elasticity				15. NUMBER OF PAGES 70
				16. PRICE CODE
17. SECURITY CLASSIFICATION OF REPORT Unclassified		18. SECURITY CLASSIFICATION OF THIS PAGE Unclassified		19. SECURITY CLASSIFICATION OF ABSTRACT Unclassified
				20. LIMITATION OF ABSTRACT UL

Approved for public release; distribution is unlimited

AN EXAMINATION OF BI-ORTHOGONALITY RELATIONSHIPS IN ELASTIC-FLUID MEDIA

Coley R. Myers, III
Lieutenant, United States Navy
B.S., North Carolina State University, 1992

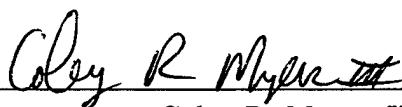
Submitted in partial fulfillment of the
requirements for the degree of

MASTER OF SCIENCE IN APPLIED MATHEMATICS

from the

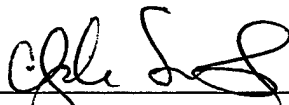
**NAVAL POSTGRADUATE SCHOOL
June 1998**

Author:

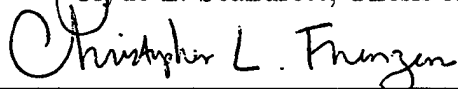


Coley R. Myers, III

Approved by:



Clyde L. Scandrett, Thesis Advisor



Christopher L. Frenzen, Thesis Co-Advisor



Walter M. Woods, Chairman
Department of Mathematics

ABSTRACT

The bi-orthogonality relationships for vertically heterogeneous porous media in contact with various surfaces have been previously established. For the special case in which the porous substance has zero porosity, the relationships reduce to those for elastic media. The bi-orthogonality relationship for a fluid loaded elastic slab will be considered numerically by discretizing the boundary value problems using finite differences. The resulting matrix will be analyzed for the purpose of determining eigenvalues of the complex dispersion relationship of the layered media, as well as discerning the corresponding eigenvectors which are discrete analogies of the propagation/evanescent eigenfunctions of the media.

TABLE OF CONTENTS

I.	INTRODUCTION	1
II.	THEORY AND METHODS	3
	A. ACOUSTIC THEORY	3
	1. Basic Acoustics and the Wave Equation	3
	2. Stress-Strain Relationships For Elastic Solids	4
	B. BI-ORTHOGONALITY	7
	C. NUMERICAL METHODS	11
	1. Newton's Method	11
	2. Finite Difference Method	12
III.	DISPERSION EQUATIONS FOR ELASTIC HALF SPACES	15
	A. INFINITE ELASTIC HALF SPACE WITH A FREE SURFACE	15
	B. FLUID LOADED INFINITE ELASTIC HALF SPACE	18
	C. FINITE FLUID INFINITE ELASTIC HALF SPACE	21
	D. FLUID LOADED ELASTIC PLATE	23
IV.	RESEARCH RESULTS	27
	A. DISCRETIZATION PROCESS	27
	B. NUMERICAL RESULTS	29
	1. Modal Wave Numbers	29
	2. Stress Potentials	31
	3. Bi-orthogonality	35
V.	CONCLUSIONS AND FUTURE RESEARCH	39
	APPENDIX. MISCELLANEOUS DATA	41
	1. MATLAB CODE FOR GENERATING WAVE SPEEDS	41
	2. DISCRETIZATION MATLAB CODE	41
	LIST OF REFERENCES	51
	INITIAL DISTRIBUTION LIST	53

LIST OF FIGURES

1.	Bi-orthogonality of Two Fluid Layers	9
2.	Infinite Free-Elastic Half Space	15
3.	Rayleigh Wave Propagation	18
4.	Infinite Fluid-Elastic Half Space	18
5.	Finite Fluid Infinite Elastic Half Space	21
6.	Fluid Loaded Elastic Plate	23
7.	Discretization of Fluid Loaded Elastic Plate	28
8.	Eigenvalues of Discretized Matrix	30
9.	Analytical versus Discretized Solutions for ϕ	32
10.	Analytical versus Discretized Solutions for φ	33
11.	Analytical versus Discretized Solutions for ψ	34
12.	Pressure - Normal Stress in Layer	36
13.	Wave Mode Propagation - Modes 1-3	37

LIST OF TABLES

I.	Rayleigh and Scholte Wave Speeds for Various Elastic Solids	23
II.	Calculated versus Refined Modal Wave Speeds	31

LIST OF ACRONYMS AND SYMBOLS

τ_{xy}	traction or shear stress in x direction
τ_{yy}	normal stress in y direction
λ	elastic constant
μ	elastic constant
c	wave speed
c_F	fluid wave speed
c_T	transverse or shear wave speed
c_L	longitudinal or compressional wave speed
c_R	Rayleigh wave speed
c_S	Scholte wave speed
p	pressure
ρ	density
β	porosity
ω	angular frequency
k	wave number
k_F	fluid wave number
k_T	transverse or shear wave number
k_L	longitudinal or compressional wave number
k_R	Rayleigh wave number
k_n	modal wave number
h_s	stepsize for solid layer
h_f	stepsize for fluid layer
E	Young's modulus
ν	Poisson's ratio
∇^2	Laplacian operator
C	denotes continuous function
C^2	space of functions with continuous second order partial derivatives

ACKNOWLEDGMENTS

I would like to extend my appreciation and gratitude to my thesis advisors, Clyde Scandrett and Chris Frenzen, for stimulating my interest in the area of acoustics. I would also like to thank them for the many discussions and constant encouragement throughout my work. In addition, their careful review of this material has definitely made for a better thesis.

I would also like to thank my parents, who have always encouraged me throughout my many endeavors. I know that I would not have achieved so much without their many years of guidance and constant support. In addition, I would also like to thank my two best friends, Wes and Noelle, who have also helped me through the years and have been a source of encouragement as well.

I. INTRODUCTION

Bi-orthogonality relationships for porous media have been developed by Professors Scandrett and Frenzen [Ref. 1]. They showed that Fraser's [Ref. 2] bi-orthogonality relationship for the propagation of Rayleigh-Lamb modes in a plate with traction-free surfaces is a special case of the porous case in which the porous slab has zero porosity. Bi-orthogonality relationships can be used to solve scattering problems from interfaces of discontinuity between vertically stratified porous/elastic/fluid media. In this thesis, we will examine the bi-orthogonality relationship for the elastic-fluid case.

Before the bi-orthogonality relationship can be used, the eigenvalues and eigenfunctions corresponding to the boundary value problem must be found. In this thesis, we will attempt to find these numerically. The question we ask ourselves is which numerical approach is the best. One method is to determine Rayleigh-Lamb modes [Ref. 3] in the elastic solid and try to perturb those solutions to obtain modes for the fluid loaded layer. The problem with this method is that modes may be missed. Another approach is to use the Rayleigh-Ritz method [Ref. 4], which is based upon the calculus of variations. It uses an expansion of elementary functions to "minimize" a functional to the corresponding boundary value problem. The functions must be carefully chosen due to the complexity of the resulting coefficient matrix which will have terms involving the unknown eigenvalues.

The method chosen in this thesis is the finite difference method. This method is very useful when numerically modeling boundary value problems involving derivatives. Using the finite difference approximations, we produce a discrete linear operator which approximates the differential operator of the boundary value problem. We can then use MATLAB [Ref. 5] to solve for eigenvalues of the linear operator which are theoretically close to the eigenvalues of the differential operator. We will also use additional numerical methods, to be discussed later, in an attempt to refine our

approximate eigenvalues.

Chapter II will provide a background in acoustical theory and will introduce terms that the reader will need to be familiar with for further chapters. Also, the concept of bi-orthogonality is explained in detail and a simple example is presented. Finally, a description of numerical techniques and methods that are used throughout the thesis will be given.

In Chapter III, background on the elastic-fluid problem is introduced. Detailed analytical solutions to several elastic half space problems are provided to establish the basis of the numerical solution. The fluid loaded plate case will be the case studied in the numerical portion of this thesis.

Chapter IV examines the numerical difference approximations used in the problem. The modal wave speeds are presented and compared to the “refined” wave speeds. Comparisons will also be made between the analytical and numerical eigenfunctions/vectors of the fluid loaded elastic plate.

Finally, Chapter V will provide conclusions and discuss areas of further research.

II. THEORY AND METHODS

A. ACOUSTIC THEORY

1. Basic Acoustics and the Wave Equation

Acoustics is generally associated with sound. However, the definition of acoustics is the generation, transmission, and reception of energy that is in the form of vibrational waves. Audible waves are between 20 and 20,000 Hz where $1\text{Hz} = 1\text{cycle/second}$. The simple oscillator[Ref. 6], or basic spring mass problem, is the most common example used to demonstrate basic acoustics. The simple oscillator is governed by the equation

$$\frac{d^2x}{dt^2} + \omega_0^2 x = 0 \quad (\text{II.1})$$

with a general solution of

$$x = A\cos(\omega_0 t) + B\sin(\omega_0 t) \quad (\text{II.2})$$

where ω_0 is the angular frequency in radians per second (rads/sec). Since there are 2π radians per cycle, we define frequency as

$$f = \frac{\omega}{2\pi}. \quad (\text{II.3})$$

In addition, we note that the period T is equal to $\frac{1}{f}$. If the initial velocity and displacement are known, we can obtain an exact solution to Equation (II.1).

The fluid-elastic problem that is the central problem of this thesis is a two-dimensional problem, and thus the fluid and elastic potential functions are governed by the two-dimensional wave equation

$$\nabla^2 \Phi = \frac{1}{c^2} \frac{\partial^2 \Phi}{\partial t^2} \quad (\text{II.4})$$

We assume an incident wave is travelling in the positive x -direction, which strikes an interface generating reflected and transmitted waves. A plane time harmonic wave propagating in the positive x -direction has the form

$$\Phi = \varphi(y)e^{-i(\omega t - k_1 x)} \quad (\text{II.5})$$

where $k_1 = \frac{\omega}{c_1}$. Substituting Equation(II.5) into Equation(II.4), one finds the amplitude function must satisfy the relation

$$\varphi''(y) + (k_1^2 - k^2)\varphi(y) = 0 \quad (\text{II.6})$$

which is the canonical form of the boundary value problem to be solved.

2. Stress-Strain Relationships For Elastic Solids

Elastic solids have the property that when external pressures are removed, the solid returns to its natural state. Strain is a measure of displacement while stress is a measure of force per area. We define the strain as

$$\varepsilon_{ij} = \frac{1}{2}(u_{i,j} + u_{j,i}) \quad (\text{II.7})$$

where u is a displacement vector and tensor notation has been adopted. The term $u_{i,j}$ means the partial derivative with respect to x_j , or for example, $u_{1,2}$ corresponds to $\frac{\partial u_1}{\partial x_2}$. The strain, ε_{ij} , corresponds to elements of a matrix. Note that ε_{ij} is dimensionless. Stress, τ_{ij} , has the dimensions of force per area. For small strain, ε , the stress, τ , is proportional to strain. This relationship is known as Hooke's Law [Ref. 7], which can be written for an isotropic homogeneous solid as

$$\tau_{ij} = \lambda \varepsilon_{kk} \delta_{ij} + 2\mu \varepsilon_{ij} \quad (\text{II.8})$$

where λ and μ , known as Lamé's elastic constants, have the dimension of pressure, and δ_{ij} is the well-known *Kronecker delta* defined as follows:

$$\delta_{ij} = \begin{cases} 1 & i = j \\ 0 & i \neq j \end{cases} \quad (\text{II.9})$$

The displacement vectors can be represented in terms of potential functions. The displacement equation of motion for an isotropic homogeneous elastic solid [Ref. 7] can be written as

$$\mu \nabla^2 \mathbf{u} + (\lambda + \mu) \nabla \nabla \cdot \mathbf{u} = \rho \ddot{\mathbf{u}} \quad (\text{II.10})$$

We consider a decomposition of the displacement vector in the form

$$\mathbf{u} = \nabla \varphi + \nabla \times \boldsymbol{\psi} \quad (\text{II.11})$$

It can be shown that the displacement vector \mathbf{u} satisfies Equation (II.10) if

$$\nabla^2 \varphi = \frac{1}{c_L^2} \ddot{\varphi} \quad (\text{II.12})$$

$$\nabla^2 \boldsymbol{\psi} = \frac{1}{c_T^2} \ddot{\boldsymbol{\psi}}$$

where $c_L^2 = \frac{\lambda + 2\mu}{\rho}$ and $c_T^2 = \frac{\mu}{\rho}$ [Ref. 7]. The question of the completeness of the solution in Equation (II.11) is guaranteed by the following theorem given in Achenbach's book on elastic solids [Ref. 7].

Completeness Theorem: Let

$$\mathbf{u} \in \mathcal{C}^2(V \times T)$$

$$\mathbf{f} \in \mathcal{C}(\mathcal{V} \times T)$$

and satisfy the equation

$$\mu \nabla^2 \mathbf{u} + (\lambda + \mu) \nabla \nabla \cdot \mathbf{u} + \rho \mathbf{f} = \rho \ddot{\mathbf{u}}$$

in a region of space V and in a closed time interval T . Also let

$$\mathbf{f} = c_L^2 \nabla F + c_T^2 \nabla \times \mathbf{G}.$$

Then there exists a scalar function $\varphi(\vec{x}, t)$ and a vector-valued function $\boldsymbol{\psi}(\vec{x}, t)$ in terms of which $\mathbf{u}(\vec{x}, t)$ is represented by

$$\mathbf{u} = \nabla \varphi + \nabla \times \boldsymbol{\psi}$$

with

$$\nabla \cdot \boldsymbol{\psi} = 0,$$

and where $\varphi(\vec{x}, t)$ and $\boldsymbol{\psi}(\vec{x}, t)$ satisfy the inhomogeneous wave equations

$$\nabla^2 \varphi + F = \frac{1}{c_L^2} \ddot{\varphi}$$

$$\nabla^2 \boldsymbol{\psi} + \mathbf{G} = \frac{1}{c_T^2} \ddot{\boldsymbol{\psi}}$$

The proof of this theorem can be found in [Ref. 7].

Representation of the displacement vector $\vec{\mathbf{u}}$ in terms of potentials will become important in the remainder of this thesis. We restrict our analysis by assuming the strain in the z direction is zero, which corresponds to the two dimensional plane strain case. This allows us to specialize our decomposition into the following

$$\begin{aligned} u &= \varphi_x + \psi_y \\ v &= \varphi_y - \psi_x \end{aligned} \tag{II.13}$$

where the vector valued displacement potential is reduced to a single nonzero scalar component. Our stress equation follows from Equation(II.8) as

$$\begin{aligned} \tau_{xy} &= \mu(u_y + v_x) \\ \tau_{yy} &= \lambda(u_x + v_y) + 2\mu v_y \end{aligned} \tag{II.14}$$

where, as before, the potentials φ and ψ satisfy Equations (II.12)

For an ideal fluid the stress in any direction equals the pressure stress of the fluid, or in equation form

$$\tau_{xx} = \tau_{yy} = -p \quad (\text{II.15})$$

B. BI-ORTHOGONALITY

We say that two functions $\varphi(x)$ and $\psi(x)$ are orthogonal over an interval $0 \leq x \leq L$, if $\int_0^L \varphi(x)\psi(x)dx = 0$. This is analogous to the dot product of two orthogonal vectors equaling zero. The orthogonality relationships[Ref. 8] for *sines* and *cosines* are as follows

$$\int_0^L \sin \frac{n\pi x}{L} \sin \frac{m\pi x}{L} dx = \begin{cases} 0 & n \neq m \\ \frac{L}{2} & n = m \end{cases} \quad (\text{II.16})$$

$$\int_0^L \cos \frac{n\pi x}{L} \cos \frac{m\pi x}{L} dx = \begin{cases} 0 & n \neq m \\ \frac{L}{2} & n = m \neq 0 \\ L & n = m = 0 \end{cases} \quad (\text{II.17})$$

$$\int_0^L \sin \frac{n\pi x}{L} \cos \frac{m\pi x}{L} dx = 0 \quad (\text{II.18})$$

This orthogonality relationship allows us to determine values of coefficients when arbitrary functions are expanded in terms of these functions. For example, if $f(x)$ can be written in the form

$$f(x) = \sum_{n=1}^{\infty} B_n \sin \frac{n\pi x}{L} \quad (\text{II.19})$$

then we can apply the orthogonality of *sines* over the interval $[0, L]$ to obtain

$$\int_0^L f(x) \sin \frac{m\pi x}{L} dx = \sum_{n=1}^{\infty} B_n \int_0^L \sin \frac{n\pi x}{L} \sin \frac{m\pi x}{L} dx \quad (\text{II.20})$$

which leads to

$$B_n = \frac{\int_0^L f(x) \sin \frac{n\pi x}{L} dx}{\int_0^L \sin^2 \frac{n\pi x}{L} dx} \quad (\text{II.21})$$

or the more familiar form

$$B_n = \frac{2}{L} \int_0^L f(x) \sin \frac{n\pi x}{L} dx \quad (\text{II.22})$$

The analysis is similar for *cosines*. Note that we have formally interchanged summation and integration in the above steps which is valid provided the series and integrals converge.

Bi-orthogonality relationships generalize the orthogonal relationships of classical eigenfunction expansions. In [Ref. 1], these relationships were derived for waves propagating at a free surface and along interfaces between porous and elastic media. The general bi-orthogonality relationship for a two dimensional porous layer which is fluid loaded is:

$$\int_{-h_2}^0 [\tau_{xx}^A u^B - \tau_{xy}^B v^A + s^A U^B]_{porous} dy + \int_0^{h_1} [-p^A U^B]_{fluid} dy = 0 \quad (\text{II.23})$$

where the fluid layer and porous layer thicknesses are h_1 and h_2 respectively, and $s = -\beta p$ where β denotes the porosity and p denotes the interstitial fluid pressure. Note also that A and B denote different modes within the same solid. When the porosity of the elastic media is zero, the equation reduces to the fluid loaded elastic solid bi-orthogonality relationship.

To illustrate how the bi-orthogonality property can be applied, we will examine the simple case of two fluids, each with different densities in contact at an interface along the y axis. In this case, the bi-orthogonality relationship reduces to standard orthogonality between sines and cosines. A diagram is shown in Figure(1),

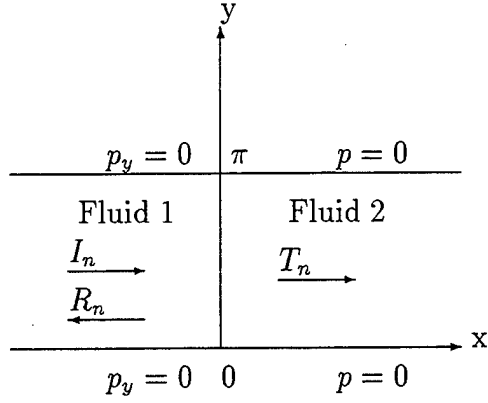


Figure 1. Bi-orthogonality of Two Fluid Layers

where fluid 1 satisfies homogeneous Neumann[Ref. 8] conditions, $p_y = 0$, and fluid 2 satisfies homogeneous Dirichlet conditions, $p = 0$, along the lateral sides of the layers. From [Ref. 8] we know the eigenfunctions are *sines* for the Dirichlet conditions and *cosines* for the Neumann conditions. We equate the pressure and flow normal to the interface to obtain

$$\begin{bmatrix} p \\ U \end{bmatrix}^1 = \sum_n \begin{bmatrix} (I_n + R_n)p_n^{(1)}(y) \\ (I_n - R_n)\frac{k_n^{(1)}}{\omega\rho_1}U_n^{(1)}(y) \end{bmatrix} = \sum_m \begin{bmatrix} T_m p_m^{(2)}(y) \\ T_m \frac{k_m^{(2)}}{\omega\rho_2}U_m^{(2)}(y) \end{bmatrix}^2 = \begin{bmatrix} p \\ U \end{bmatrix}^2 \quad (\text{II.24})$$

where $p_n^{(j)}(y)$ and $U_n^{(j)}(y)$ are defined as follows:

$$\begin{aligned} p_n^{(1)}(y) &= \cos(ny) \quad \text{and} \quad p_m^{(2)}(y) = \sin(my) \\ U_n^{(1)}(y) &= \cos(ny) \quad \text{and} \quad U_m^{(2)}(y) = \sin(my) \end{aligned} \quad (\text{II.25})$$

Applying the bi-orthogonality condition as follows

$$\begin{aligned} &\int_0^\pi U_i^{(1)}[p^1 = p^2]dy \\ &\int_0^\pi p_i^{(1)}[U^1 = U^2]dy \\ &\int_0^\pi U_i^{(2)}[p^1 = p^2]dy \\ &\int_0^\pi p_i^{(2)}[U^1 = U^2]dy, \end{aligned} \quad (\text{II.26})$$

we obtain the following two sets of equations, written in matrix form for easier manipulation

$$\begin{aligned}\mathbf{J}(\vec{I} + \vec{R}) &= \mathbf{K}\vec{T}, \\ \mathbf{J}(\vec{I} - \vec{R}) &= \mathbf{G}^T\vec{T},\end{aligned}\tag{II.27}$$

$$\begin{aligned}\mathbf{G}(\vec{I} + \vec{R}) &= \mathbf{Q}\vec{T}, \\ \mathbf{K}^T(\vec{I} - \vec{R}) &= \mathbf{Q}\vec{T}.\end{aligned}$$

We now define $\mathcal{G} = (\mathbf{Q}^{-1}\mathbf{G})$ and $\mathcal{K} = (\mathbf{J}^{-1}\mathbf{K})$, which, if both formulations are to give identical answers, results in an identity $\mathcal{G}\mathcal{K} = I$. Solving for \mathcal{G} and \mathcal{K} we have:

$$\mathcal{G}_{pn} = (\mathbf{Q}^{-1}\mathbf{G}) = \frac{\int_0^\pi \cos(py)\sin(ny)dy}{\int_0^\pi \sin^2(ny)dy}\tag{II.28}$$

$$\mathcal{K}_{nq} = (\mathbf{J}^{-1}\mathbf{K}) = \frac{\int_0^\pi \cos(qy)\sin(ny)dy}{\int_0^\pi \cos^2(qy)dy}$$

leading to

$$\mathcal{G}_{pn} = \frac{4}{\pi} \left(\frac{n}{n^2 - (p-1)^2} \right) \quad \text{where } p+n \text{ must be even}\tag{II.29}$$

$$\mathcal{K}_{nq} = \frac{2(2 - \delta_{q1})}{\pi} \left(\frac{n}{n^2 - (q-1)^2} \right) \quad \text{where } q+n \text{ must be even,}$$

which gives the matrix element $(\mathcal{G}\mathcal{K})_{qp}$ as

$$\sum_n \mathcal{G}_{pn}\mathcal{K}_{nq} = \begin{cases} 0 & \text{if } p+q \text{ is odd} \\ \frac{8(2 - \delta_{q1})}{\pi^2} \sum_n \frac{n^2}{[n^2 - (p-1)^2][n^2 - (q-1)^2]} & \text{if } p+q \text{ is even.} \end{cases}\tag{II.30}$$

It can be shown that the above summation gives

$$(\mathcal{GK})_{pq} = \delta_{pq} \quad (\text{II.31})$$

Knowing these relationships and given initial incident wave amplitudes, \vec{I} , we can solve for the reflected and transmitted amplitudes from either one of the pairs of vector equations given by Equations (II.27).

C. NUMERICAL METHODS

1. Newton's Method

Newton's method, one of the numerical methods used in this thesis, is a widely used method for solving nonlinear equations. We will briefly review the concepts and give a short example of this method. Newton's Method uses a line tangent to the curve of a function and is based on the linear approximation of the function. We start with an initial guess x_0 , that we believe to be close to the root, and determine $f(x_0)$. Then we move along the tangent line until the point intersects the x -axis. This value of x now becomes our next iterate. In general terms, Newton's Method is given as [Ref. 4]

$$x_{n+1} = x_n - \frac{f(x_n)}{f'(x_n)} \quad (\text{II.32})$$

where $n = 0, 1, 2, \dots$. Newton's Method converges rapidly when the initial guess is in the neighborhood of the root. In fact, Newton's Method is quadratically convergent. Here is an example [Ref. 4]:

$$f(x) = 3x + \sin x - e^x$$

$$f'(x) = 3 + \cos x - e^x$$

We choose $x_0 = 0$ and perform 3 iterations as follows

$$x_1 = x_0 - \frac{f(x_0)}{f'(x_0)} = .33333$$

$$x_2 = x_1 - \frac{f(x_1)}{f'(x_1)} = .36017$$

$$x_3 = x_2 - \frac{f(x_2)}{f'(x_2)} = .3604217$$

which is accurate to 7 significant digits. Although the convergence is rapid, there are other considerations that need to be addressed with this method. Newton's Method requires 2 function evaluations per step. However, the total number of function evaluations is generally the same or less than other methods and Newton's Method usually takes fewer iterations to determine a root with high accuracy. The main drawback to Newton's Method is that it will not converge for certain functions. This happens when the tangent line is approximately horizontal or when we repeat a value previously used, for example $x_1 = x_4$. Although these are strong considerations, this happens infrequently. For our needs, we will use this method to refine our wave speeds found in Chapter III. We will also use this method in refining our eigenvalue estimates found using the finite difference method which is discussed in Chapter IV.

2. Finite Difference Method

The finite difference method is used in numerically approximating derivatives and integrals of functions. We can use this ability to replace derivatives with difference quotients and thereby approximate solutions to difficult differential equations. There are three basic types of difference quotients; backward, central, and forward, with central being the most accurate. In certain instances, such as endpoints, backward or forward differences are often used due to the lack of additional points beyond the extremity of an interval necessary for accomplishing the central difference. In any case, it is customary to ensure that all difference operators have the same or like order of accuracy to avoid extra work and increase the possibility of error cancellation. Difference operators can also be applied more than once in order to obtain second order and higher difference approximations to higher order derivatives. For this thesis, we will concern ourselves with only second order differences. The central difference operators [Ref. 4] are as follows:

$$\frac{dx}{dt}\bigg|_{t=t_i} = \frac{x_{i+1} - x_{i-1}}{2h} + O(h^2) \quad (\text{II.33})$$

$$\frac{d^2x}{dt^2}\bigg|_{t=t_i} = \frac{x_{i+1} - 2x_i + x_{i-1}}{h^2} + O(h^2)$$

where $h = \Delta x$ is the stepsize. Since forward and backward differences are $O(h)$, we need to expand x_{i+1} and x_{i-1} as follows to obtain formulas of higher order for our backward and forward difference operators:

$$\begin{aligned} x_{i+1} &= x_i + x'_i h + x''_i h^2 + x'''_i h^3 + \dots \\ x_{i-1} &= x_i - x'_i h + x''_i h^2 - x'''_i h^3 + \dots \end{aligned} \quad (\text{II.34})$$

Re-arranging terms we obtain

$$\begin{aligned} x'_i &= \frac{x_{i+1} - x_i}{h} - \frac{h}{2}x''_i - \frac{h^2}{6}x'''_i + O(h^3) && \text{forward difference} \\ x'_i &= \frac{x_i - x_{i-1}}{h} + \frac{h}{2}x''_i - \frac{h^2}{6}x'''_i + O(h^3) && \text{backward difference} \end{aligned} \quad (\text{II.35})$$

We will be able to substitute for the terms x''_i , and x'''_i in our final discretization. This will be discussed in more detail in Chapter IV.

III. DISPERSION EQUATIONS FOR ELASTIC HALF SPACES

In this chapter we will examine several elastic fluid problems with infinite and finite layers. In each problem a relationship known as the Dispersion Equation is found. A system is dispersive if the phase velocity of a wave depends upon the frequency of the wave. Solving this dispersion relationship at a prescribed frequency, we can determine the wavespeeds for propagating modes and use this for an analysis of the system. These modes are also the necessary constituents in applying the bi-orthogonality relationships being studied.

A. INFINITE ELASTIC HALF SPACE WITH A FREE SURFACE

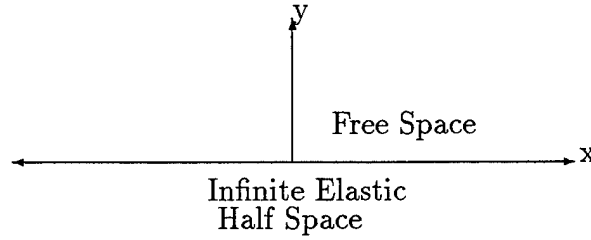


Figure 2. Infinite Free-Elastic Half Space

The case of an infinite elastic half space with a free surface is described by Achenbach [Ref. 7]. We consider the two dimensional plane strain case. We apply stress free boundary conditions at the free surface:

$$\tau_{xy} = \mu(u_y + v_x) = 0 \quad (\text{III.1})$$

$$\tau_{yy} = \lambda(u_x + v_y) + 2\mu v_y = 0 \quad (\text{III.2})$$

Dividing Equation (III.2) by ρ and substituting our longitudinal and transverse wave speeds, c_L^2 and c_T^2 we obtain

$$c_L^2 v_y + (c_L^2 - 2c_T^2) u_x = 0 \quad (\text{III.3})$$

Assuming a solution for our vector potentials, φ and ψ , as follows,

$$\begin{aligned} \varphi &= \tilde{\varphi}(y) e^{-i(\omega t - kx)} \\ \psi &= \tilde{\psi}(y) e^{-i(\omega t - kx)} \end{aligned} \quad (\text{III.4})$$

our solutions for u and v become

$$\begin{aligned} u &= \varphi_x + \psi_y = ik\varphi + \psi_y \\ v &= \varphi_y - \psi_x = \varphi_y - ik\psi \end{aligned} \quad (\text{III.5})$$

and the two boundary conditions can be written:

$$\begin{aligned} u_y + ikv &= 0 \\ (c_L^2 - 2c_T^2)iku + c_L^2 v_y &= 0 \end{aligned} \quad (\text{III.6})$$

Next, our potential functions must solve Helmholtz equations in the elastic solid,

$$\begin{aligned} \nabla^2 \varphi + k_L^2 \varphi &= 0 \\ \nabla^2 \psi + k_T^2 \psi &= 0 \end{aligned} \quad (\text{III.7})$$

Dropping the tilde notation on the “amplitude” functions of y and the $e^{-i(\omega t - kx)}$ dependence, these functions satisfy the wave equation if

$$\begin{aligned} \varphi'' - \eta^2 \varphi &= 0, \\ \psi'' - \xi^2 \psi &= 0, \end{aligned} \quad (\text{III.8})$$

where $\eta^2 = k^2 - k_L^2$ and $\xi^2 = k^2 - k_T^2$. This leads to exponential solutions

$$\begin{aligned} \varphi &= Ae^{-\eta y} + Be^{\eta y} \\ \psi &= Ce^{-\xi y} + De^{\xi y} \end{aligned} \quad (\text{III.9})$$

where we stipulate that $Re(\xi, \eta) > 0$. To ensure boundedness of the solutions as $y \rightarrow -\infty$, we neglect solutions that “blow up” to obtain

$$\begin{aligned}\varphi &= Be^{\eta y} \\ \psi &= De^{\xi y}\end{aligned}\tag{III.10}$$

Substituting into the boundary conditions we have

$$\begin{aligned}ik\eta\varphi + \xi^2\psi + ik(\eta\varphi - ik\psi) &= 0 \\ (c_L^2 - 2c_T^2)ik(ik\varphi + \xi\psi) + c_L^2(\eta^2\varphi - ik\xi\psi) &= 0\end{aligned}\tag{III.11}$$

Evaluating the amplitude functions at $y = 0$ and simplifying leads to

$$\begin{aligned}(2k^2 - k_T^2)B - 2ik\xi D &= 0 \\ 2ik\eta B + (2k^2 - k_T^2)D &= 0\end{aligned}\tag{III.12}$$

The determinant of the coefficient matrix in Equation (III.12) leads to the Dispersion Equation

$$(2k^2 - k_T^2)^2 - 4k^2\xi\eta = 0\tag{III.13}$$

In this instance, the waves are nondispersive because the phase speed determined by the above relationship is independent of the frequency. The frequency can be scaled out by noting $k = \frac{\omega}{c}$, and dividing the equation by ω^4 . Using $c_L = 5690m/s$ and $c_T = 3145m/s$, the compressional and shear wave speeds for *steel*, we can apply Newton's Method to solve for c_R , the Rayleigh wave speed, and find

$$c_R = 2907m/s$$

where $c_R < c_T < c_L$. From [Ref. 7] we have the following approximate formula for computing the Rayleigh wave speed.

$$c_R \approx \frac{.862 + 1.14\nu}{1 + \nu}c_T\tag{III.14}$$

Using this formula, we predict a Rayleigh wave speed of $2902.25m/s$ which is very close to our result. Now letting $D = 1$ we find that $B = .6748i$. At the frequency $\omega = 1$ and setting $x = y = 0$, the real parts of the particle displacements (u, v) have been plotted in Figure(3). Note that this is the time history of the particle displacement at the surface of the elastic half space. In addition, as depth increases, the amplitude of the Rayleigh wave decreases and the motion alternates between retrograde and prograde. Rayleigh waves for various elastic solids appear in Table (I) later in this chapter.

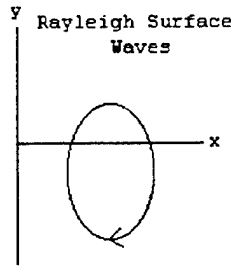


Figure 3. Rayleigh Wave Propagation

B. FLUID LOADED INFINITE ELASTIC HALF SPACE

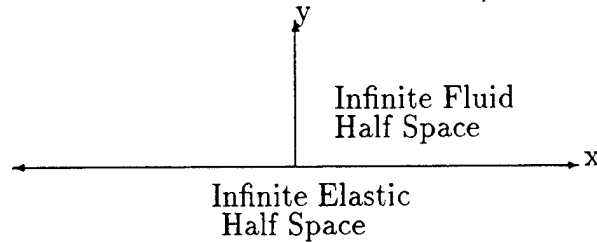


Figure 4. Infinite Fluid-Elastic Half Space

When a fluid is added, we have slightly different boundary conditions. Equation (III.1) still holds, but Equation (III.2) is modified due to the fluid pressure at

the boundary. This leads to

$$\tau_{yy} = \lambda(u_x + v_y) + 2\mu v_y = -p \quad (\text{III.15})$$

for which

$$p = -\rho_f \phi_t \quad (\text{III.16})$$

and where ϕ is the acoustic velocity potential for the fluid and ρ_f is the fluid density.

The normal stress boundary condition becomes

$$c_L^2 v_y + (c_L^2 - 2c_T^2)u_x + i\omega \frac{\rho_f}{\rho_s} \phi = 0 \quad (\text{III.17})$$

We allow slippage along the fluid/solid interface ($y = 0$), but demand continuity of the vertical velocity there, i.e. $v_{solid} = v_{fluid}$. This leads to a third boundary condition

$$-i\omega \varphi_y - \omega k \psi + \phi_y = 0 \quad (\text{III.18})$$

The velocity potential function must also satisfy a Helmholtz equation

$$\nabla^2 \phi + k_F^2 \phi = 0 \quad (\text{III.19})$$

where $k_F = \frac{\omega}{c_F}$ and c_F is the fluid wave speed. As before we determine the form of our solution using the wave equation and assuming a potential of the form

$$\phi = \tilde{\phi}(y) e^{-i(\omega t - kx)} \quad (\text{III.20})$$

Dropping again the tilde notation and the $e^{-i(\omega t - kx)}$ dependence, the amplitude function must satisfy

$$\phi_{yy} - \zeta^2 \phi = 0 \quad (\text{III.21})$$

where $\zeta^2 = k^2 - k_F^2$. The amplitude function has the exponential solution

$$\phi = Ee^{-\zeta y} + Fe^{\zeta y} \quad (\text{III.22})$$

Disregarding solutions that “blow up” as $y \rightarrow \pm\infty$ we obtain the amplitude functions for the solid and fluid

$$\begin{aligned} \varphi &= Be^{\eta y} \\ \psi &= De^{\xi y} \\ \phi &= Ee^{-\zeta y} \end{aligned} \quad (\text{III.23})$$

Substituting these into the three boundary conditions we have at $y = 0$:

$$\begin{aligned} 2ik\eta\varphi + (\xi^2 + k^2)\psi &= 0 \\ (c_L^2\eta^2 - k^2(c_L^2 - 2c_T^2))\varphi - 2ik\xi c_T^2\psi + i\omega\frac{\rho_f}{\rho_s}\phi &= 0 \\ i\omega\eta\varphi + \omega k\psi - \zeta\phi &= 0 \end{aligned} \quad (\text{III.24})$$

Simplifying we obtain

$$\begin{aligned} 2ik\eta B + (2k^2 - k_T^2)D &= 0 \\ (2k^2 c_T^2 - k_L^2 c_L^2)B - 2ik\xi c_T^2 D + i\omega\frac{\rho_f}{\rho_s}E &= 0 \\ i\omega\eta B + \omega kD - \zeta E &= 0 \end{aligned} \quad (\text{III.25})$$

Computing the determinant of the matrix and simplifying results in the Dispersion Equation. However, unlike the previous case, we now have an added term due to the presence of the fluid half space. This equation is

$$[(2k^2 - k_T^2)^2 - 4k^2\eta\xi] + k_T^4\frac{\eta}{\zeta}\frac{\rho_f}{\rho_s} = 0 \quad (\text{III.26})$$

Note that once again the frequency can be factored out of the above expression which implies a nondispersive media. Applying Newton’s Method using the wave speeds for *steel* we determine what is referred to as the Scholte[Ref. 7] wave speed,

$$c_s = 2903.567 - 35.325i \quad m/s$$

Note that in the case with the fluid half space we have a complex wave speed. Letting $E = 1$ we find $B = 2.51 + .395i$ and $D = -.030 + 3.89i$. Setting $\omega = 1$ and plotting the real part of the horizontal and vertical displacements at $x = y = 0$, we obtain the particle displacement history as this Scholte wave passes through the point $x = y = 0$. The plot looks the same as Figure (3).

C. FINITE FLUID INFINITE ELASTIC HALF SPACE

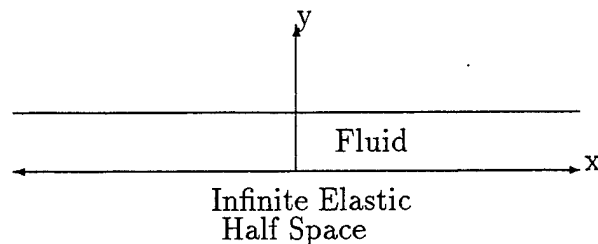


Figure 5. Finite Fluid Infinite Elastic Half Space

We next consider a fluid layer of finite thickness overlying an elastic half space. The boundary conditions from before, Equations (III.15), (III.17), and (III.18) still hold. However, an additional boundary condition is needed at the boundary between the fluid and free space which is that the pressure be zero there. From Equation (III.16), this leads to

$$p = i\omega\rho_f\phi = 0 \Rightarrow \phi = 0 \quad (\text{III.27})$$

Also, from before we obtain the solutions to the Helmholtz equation where

$$\begin{aligned} \varphi &= Ae^{\eta y} \\ \psi &= Be^{\xi y} \end{aligned} \quad (\text{III.28})$$

Our third potential changes because we now have a finite layer. We are unable to discard one of the solutions, but instead must have

$$\phi = Ce^{\zeta y} + De^{-\zeta y} \quad (\text{III.29})$$

Simplifying this by combining the terms, we choose

$$\phi = C \sinh(\zeta(h - y)) \quad (\text{III.30})$$

Notice that by making this choice we have incorporated our additional boundary condition so that when $y = h$, $\phi = 0$. Substituting into the boundary conditions at $y = 0$, we have

$$\begin{aligned} 2ik\eta\varphi + (\xi^2 + k^2)\psi &= 0 \\ (c_L^2\eta^2 - k^2(c_L^2 - 2c_T^2))\varphi - 2ik\xi c_T^2\psi + i\omega\frac{\rho_f}{\rho_s}\phi &= 0 \\ i\omega\eta\varphi + \omega k\psi - \zeta C \cosh(\zeta(h - y)) &= 0 \end{aligned} \quad (\text{III.31})$$

or

$$\begin{aligned} 2ik\eta A + (2k^2 + k_T^2)B &= 0 \\ (2k^2 c_T^2 - \omega^2)A - 2ik\xi c_T^2 B + i\omega\frac{\rho_f}{\rho_s} \sinh(\zeta h)C &= 0 \\ i\omega\eta A + \omega k B - \zeta \cosh(\zeta h)C &= 0 \end{aligned} \quad (\text{III.32})$$

Computing the determinant and simplifying leads us again to a Dispersion Equation, which is

$$\left[(2k^2 - k_T^2)^2 - 4k^2\eta\xi \right] + k_T^4 \frac{\eta}{\zeta} \frac{\rho_f}{\rho_s} \tanh(\zeta h) = 0 \quad (\text{III.33})$$

Unlike the previous case, the frequency can no longer be factored out. This dispersion relation signals that we now have a dispersive media which is intermediate between the other two limiting cases. Notice that as $\omega \rightarrow 0$, the “fluid term” is $O(\omega^5)$ while the solid terms are $O(\omega^4)$, and therefore the wave acts like a Rayleigh wave. As $\omega \rightarrow \infty$, $\tanh(\zeta h) \rightarrow 1$ we obtain the Scholte limit. This makes sense physically because as $\omega \rightarrow 0$, $\lambda \sim O(\frac{1}{\omega})$ becomes large and the fluid layer will appear to become extremely “thin” relative to the propagating wavelength. On the other hand if $\omega \rightarrow \infty$, the

fluid will appear to be "thicker" in terms of the number of wavelengths that can fit onto the fluid layer, and we get the other limit of an infinite fluid layer. As in the previous problems we solve for the Scholte interface wave speed. A height of $1m$ is used for the fluid layer in the computation. The wave speed for *steel* is

$$c = 2906 - .0011i \text{ m/s}$$

Letting $C = 1$ we find that $A = .00947 - .104x10^{-8}i$ and $B = .147x10^{-8} - .00571i$. We now set $\omega = 1$, $h = 1$, and $x = y = 0$. This plot is the same as our Rayleigh wave plot in Figure (3), which was expected. Listed below in Table (I) are Rayleigh and Scholte wave speeds for various elastic solids.

Solid	c_L	c_T	c_R	$c_{S_{infinitefluid}}$	$c_{S_{finitefluid}}$
Steel	5690	3145	2907	$2904 - 35i$	$2906 - .001i$
Iron (Cast)	4175	2308	2133	$2127 - 45i$	$2133 - .0009i$
Aluminum	6242	3144	2930	$2904 - 112i$	$2930 - .003i$
Glass (Pyrex)	5637	3297	3026	$2993 - 153i$	$3026 - .004i$
Rubber (Hard)	2117	864	814	694	814

Table I. Rayleigh and Scholte Wave Speeds for Various Elastic Solids

D. FLUID LOADED ELASTIC PLATE

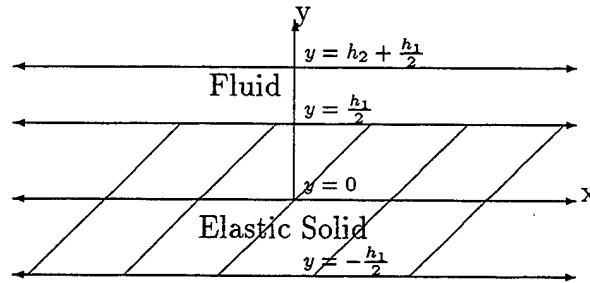


Figure 6. Fluid Loaded Elastic Plate

We consider an elastic layer of finite thickness. We examine the relationship of a finite fluid media in contact with a finite elastic medium or plate. As shown

in Figure (6), the origin is assumed to go through the middle of the elastic solid. This will help later to show the symmetric and anti-symmetric modes as discussed by Achenbach [Ref. 7] in the unloaded, "free plate" problem. Our boundary conditions are slightly different with this case. We choose a thickness h_1 for the elastic layer and a thickness h_2 for the fluid layer. At $y = -\frac{h_1}{2}$ we have

$$\begin{aligned}\tau_{xy} &= 0 \\ \tau_{yy} &= 0\end{aligned}\tag{III.34}$$

At $y = +\frac{h_1}{2}$, we have

$$\begin{aligned}\tau_{xy} &= 0 \\ \tau_{yy} &= -p \\ v_{solid} &= v_{fluid}\end{aligned}\tag{III.35}$$

Finally, at $y = h_2 + \frac{h_1}{2}$, we want the pressure to again be equal to zero. We again assume solutions to the wave equation. However, we now have a finite fluid and elastic layer, and therefore must retain all of the exponential terms. We write the solutions in terms of cosh and sinh in order to better see the symmetric and anti-symmetric portions of the solutions. We have,

$$\begin{aligned}\varphi &= A \cosh(\eta y) + B \sinh(\eta y) \\ \psi &= C \cosh(\xi y) + D \sinh(\xi y) \\ \phi &= E \sinh(\zeta(h - y))\end{aligned}\tag{III.36}$$

where $h = \frac{h_1}{2} + h_2$, and we have taken into account the boundary condition that $p = 0$ at h .

Substituting into our boundary conditions and letting $\rho = \frac{\rho_f}{\rho_s}$, we have

$$\begin{aligned}
2ik\eta\varphi_y(-\frac{h_1}{2}) + (2k^2 - k_T^2)\psi(-\frac{h_1}{2}) &= 0 \\
2ik\eta\varphi_y(\frac{h_1}{2}) + (2k^2 - k_T^2)\psi(\frac{h_1}{2}) &= 0 \\
(2k^2 - k_T^2)\varphi(-\frac{h_1}{2}) - 2ik\xi\psi_y(-\frac{h_1}{2}) &= 0 \\
(2k^2 - k_T^2)\varphi(\frac{h_1}{2}) - 2ik\xi\psi_y(\frac{h_1}{2}) + \frac{ik_T\rho}{c_T}\phi(h_2) &= 0 \\
i\omega\eta\varphi_y(\frac{h_1}{2}) + \omega k\psi(\frac{h_1}{2}) - \phi_y(h_2) &= 0
\end{aligned} \tag{III.37}$$

Trying to find and simplify the determinant is difficult. We try a simpler approach by adding and subtracting like equations to obtain our Dispersion Equation. Adding and subtracting the first two equations and doing the same with the next two equations, we have the following

$$\begin{aligned}
2ik\eta B \cosh(\eta\frac{h_1}{2}) + (2k^2 - k_T^2)C \cosh(\xi\frac{h_1}{2}) &= 0 \\
2ik\eta A \sinh(\eta\frac{h_1}{2}) + (2k^2 - k_T^2)D \sinh(\xi\frac{h_1}{2}) &= 0 \\
(2k^2 - k_T^2)A \cosh(\eta\frac{h_1}{2}) - 2ik\xi D \cosh(\xi\frac{h_1}{2}) + \frac{ik_T\rho}{2c_T}E \sinh(\zeta h_2) &= 0 \\
(2k^2 - k_T^2)B \sinh(\eta\frac{h_1}{2}) - 2ik\xi C \sinh(\xi\frac{h_1}{2}) + \frac{ik_T\rho}{2c_T}E \sinh(\zeta h_2) &= 0 \\
i\omega\eta\varphi_y(\frac{h_1}{2}) + \omega k\psi(\frac{h_1}{2}) - \phi_y(h_2) &= 0
\end{aligned} \tag{III.38}$$

From the first two equations, we solve for A and B in terms of C and D . Substituting into the next two equations we obtain a relationship of C and D and find E in terms of C . This is not as difficult as it seems, but does require accurate bookkeeping to keep up with the algebra. Substituting all of these into the last equation, and after much algebra, we obtain the Dispersion Equation for a fluid loaded plate.

$$\begin{aligned}
&[(2k^2 - k_T^2)^2 - 4k^2\eta\xi \tanh(\eta\frac{h_1}{2}) \coth(\xi\frac{h_1}{2})][(2k^2 - k_T^2)^2 - 4k^2\eta\xi \coth(\eta\frac{h_1}{2}) \tanh(\xi\frac{h_1}{2})] \\
&= \frac{-\rho_f k_T^4 \eta \tanh(\zeta h_2)}{\rho_s \zeta} [(2k^2 - k_T^2)^2 \coth(\eta h_1) - 4k^2\eta\xi \coth(\xi h_1)]
\end{aligned} \tag{III.39}$$

Because the dispersion relationships will involve infinitely many complex roots, due to the finite nature of the elastic/fluid system, Newton's method may indeed be able to find one or several of the roots, but will not be efficient in finding the first N roots

(ordered by magnitude), simply because required starting values are not available. One lacks the confidence that all of the eigenvalues will be found with Newton's method without sufficiently close starting values.

IV. RESEARCH RESULTS

A. DISCRETIZATION PROCESS

We begin the numerical analysis of the fluid loaded plate by applying finite difference approximations to the boundary value problem. We know that in the fluid and solid, the respective reduced Helmholtz equations must be satisfied. We define $(N + 1)h_f$ as the thickness of the fluid layer and $(M + 1)h_s$ as the thickness for the elastic layer, where $(N + 1)$ is the number of discrete points in the fluid layer and $(M + 1)$ as the number of grid points in the elastic layer, and h_f and h_s are the stepsize for the fluid and elastic layers, respectively. In order to obtain our unknown modal wave number, k_n^2 , on the right hand side of the system of equations, several substitutions are necessary. We define $\psi^* = \psi_x$, and also substitute $\phi_t = \phi$. Therefore in the final analysis we will be solving for normal modes of the functions ϕ_t, φ , and ψ^* . Dropping the superscripts and subscripts to avoid clutter in the discretization, we have

$$\begin{aligned} \phi_i'' + k_f^2 \phi_i &= k_n^2 \phi_i & i &= 1..N - 1 \\ \varphi_i'' + k_L^2 \varphi_i &= k_n^2 \varphi_i & i &= 1..M - 1 \\ \psi_i'' + k_T^2 \psi_i &= k_n^2 \psi_i & i &= 1..M - 1 \end{aligned} \quad (IV.1)$$

The additional boundary conditions on the fluid loaded elastic plate from Chapter III, can be reduced after completing the above substitutions and applying the finite difference method, to the following:

$$\begin{aligned} \phi_N &= 0 \\ 2\varphi'' + (2k_L^2 - k_T^2)\varphi - 2\psi' &= \frac{\rho_L}{\mu}\phi \\ -2k_n^2\varphi' + k_T^2\psi + 2\psi'' &= 0 \\ \psi - \varphi' &= \frac{\phi'}{\omega^2} \\ 2\varphi'' + (2k_L^2 - k_T^2)\varphi - 2\psi' &= 0 \\ -2k_n^2\varphi' + k_T^2\psi + 2\psi'' &= 0 \end{aligned} \quad (IV.2)$$

where $i = 0$ is the interface between the fluid and the solid. In order to incorporate these additional boundary conditions into Equations (IV.1), we must solve for what we will call, *pseudo nodes*. A pseudo node is a point outside of the fluid or elastic solid that will be used in the differencing of a potential. This can be seen below in Figure (7),

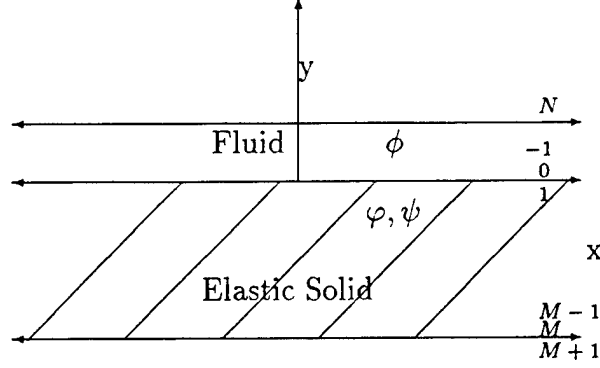


Figure 7. Discretization of Fluid Loaded Elastic Plate

where ϕ_1 is the pseudo node for the fluid and $\varphi_{-1}, \psi_{-1}, \varphi_{M+1}$, and ψ_{M+1} are the pseudo nodes for the elastic solid.

The equations for the pseudo nodes require some careful algebra and can be reduced to the following:

$$\begin{aligned}
 \phi_1 &= \phi_{-1} + \frac{h_s h_f \omega^2 \rho_f}{\mu} \phi_0 + \frac{k_T^2 h_s^2 h_f \omega^2}{2} \psi_0 - 2h_f \omega^2 \psi_1 + \frac{h_f \omega^2}{h_s} [1 + h_s^2 (k_T^2 - k_L^2)] \varphi_0 - h_s h_f k_L^2 \omega^2 \varphi_1 - \frac{h_f \omega^2}{h_s} \varphi_2 \\
 \varphi_{-1} &= [1 + h_s^2 (k_T^2 - k_L^2)] \varphi_0 + (1 - h_s^2 k_L^2) \varphi_1 - \varphi_2 + (2h_s + \frac{k_T^2 h_s^3}{2}) \psi_0 - 2h_s \psi_1 + \frac{h_s^2 \rho_f}{\mu} \phi_0 \\
 \psi_{-1} &= (4 + k_T^2 h_s^2) \psi_0 - 3\psi_1 + (h_s k_T^2 - \frac{2}{h_s}) \varphi_0 + (\frac{4}{h_s} - 2k_L^2 h_s) \varphi_1 - \frac{2}{h_s} \varphi_2 + \frac{h_s \rho_f}{\mu} \phi_0 \\
 \varphi_{M+1} &= [1 - h_s^2 (k_L^2 - k_T^2)] \varphi_M + (1 - h_s^2 k_L^2) \varphi_{M-1} - \varphi_{M-2} + 2h_s \psi_{M-1} + (\frac{h^3 k_T^2}{2} - 2h_s) \psi_M \\
 \psi_{M+1} &= (4 - h_s^2 k_T^2) \psi_M - 3\psi_{M-1} + (\frac{2}{h_s} - h_s k_T^2) \varphi_M + (2k_L^2 h_s - \frac{4}{h_s}) \varphi_{M-1} + \frac{2}{h_s} \varphi_{M-2}
 \end{aligned} \tag{IV.3}$$

These pseudo nodes are substituted into our Helmholtz equations from (IV.1) to obtain equations for the boundaries $i = 0$ and $i = M$. Our discretized boundary equations are now entered into a MATLAB code given in the Appendix. Note that for the MATLAB code we must start our index at 1 as MATLAB does not have 0 indices. A shift is required so that the first N places correspond to ϕ , the next $M + 1$

places correspond to φ , and lastly, the next $M + 1$ places correspond to ψ . This allows us to keep track of each of the three potentials. MATLAB computes our eigenvalues and orders them in ascending magnitude. The code also calculates the normal and shear stresses for use in applying the bi-orthogonality condition. Finally, various graphs involving our discretized solutions will be plotted against analytical solutions. The analytical solutions for stresses, pressures, and displacements are determined using the coefficients listed in the last section of Chapter III.

B. NUMERICAL RESULTS

1. Modal Wave Numbers

The elastic solid used for the following analysis will be *steel*. We begin with an examination of the eigenvalues of our discretized matrix. In the discretization, $\omega = 2\pi$, $N = 10$, and $M = 50$, leading to a square matrix of size 112 from which 112 eigenvalues are determined. Since we are solving for k_n^2 , we must take the square root of the eigenvalues and place them in order. Determination of the accuracy of these wave numbers will involve substitution into Equation (III.39), our fluid loaded elastic plate dispersion relation. A plot of the norm of the eigenvalues is shown in Figure (8) on the following page. Aside from the last few eigenvalues, we get a nice ordering of the eigenvalues.

We attempt to refine our approximate wave numbers using several iterations of MAPLE coded Newton's Method with the eigenvalues as initial iterates. The results are shown in Table (II). For some of our "refined" wave speeds, Newton's Method attempts to converge to a root. Newton's Method diverged for the roots marked with an asterik. After refinement, several of the roots show improvement in satisfying this equation, i.e. the magnitude of the residual of the relationship is much closer to zero. The fundamental root has a residual magnitude change from 10^{-23} to 10^{-50} . The second and third roots change almost as much. However, the rest of the roots exhibit less of a change in magnitude, indicating that the starting values for the roots may

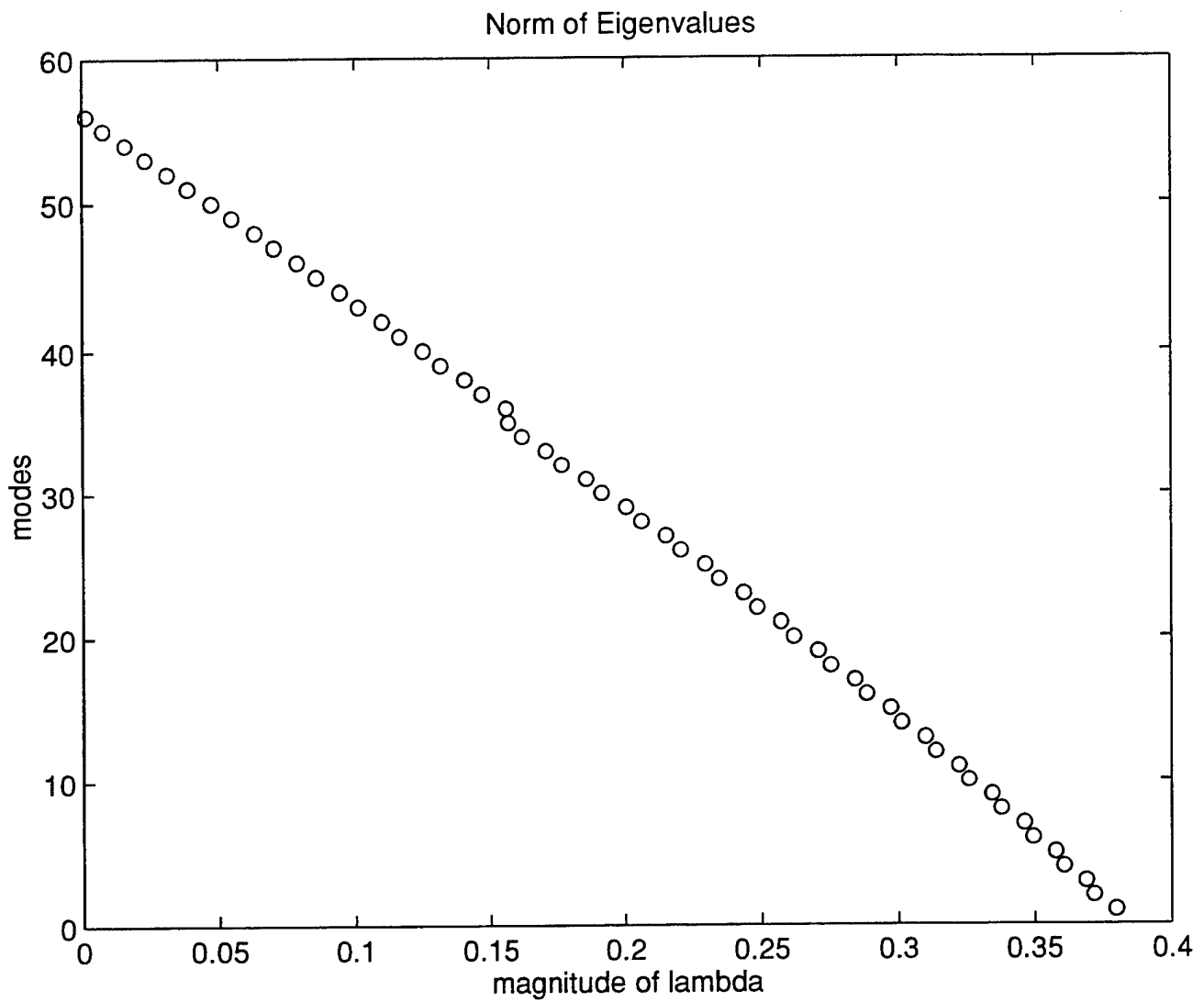


Figure 8. Eigenvalues of Discretized Matrix

not be close enough to the actual roots for Newton's Method to converge.

n	k_n	Refined k_n	relative error
1	.001291 - .0003723i	.001218	0.2824
2	.001291 + .0003723i	.001218	0.2824
3	.008880	.004932	.4445
4	.006711 - .008003i*	————	————
5	.006711 + .008003i*	————	————
6	.004703 - .01666i*	————	————
7	.004703 + .01666i*	————	————
8	.002550 - .0318i	.01127 - .0210i	.4355
9	.002550 + .0318i	.01127 + .0210i	.4355
10	.001664 - .0476i	.0007991 - .0398i	.1646

Table II. Calculated versus Refined Modal Wave Speeds

Table (II) shows the first three roots converging to a real root. The other "refined" k_n 's do not appear to converge to any of the k_n 's used as initial starting values. It may be necessary to search more than the first ten modes to help determine if a shift of the "refined" values to a corresponding k_n is possible. For this reason, we will concentrate on the first few modes.

2. Stress Potentials

The following graphs show the analytical versus the discretized solutions for the fluid and solid potentials ϕ , φ , and ψ . Figure (9), displays the best results. The analytical solution of ϕ is almost identical with the discretized solution. Note that the discretization code has ϕ_1 as the first interior point and not the boundary. This accounts for the slight mismatch at the fluid-free space boundary. Figure (10) shows a similar pattern where our solution is nearly identical, but diverges slightly as we near the fluid-elastic boundary. Figure (11) diverges at both ends but is on a scale of 10^{-5} . When viewed on a small scale, the discretized solution does diverge more than ϕ and φ . It is obvious that there is a problem at the fluid-elastic boundary and from Figure (11), there is a slight indication of a problem at the bottom boundary.

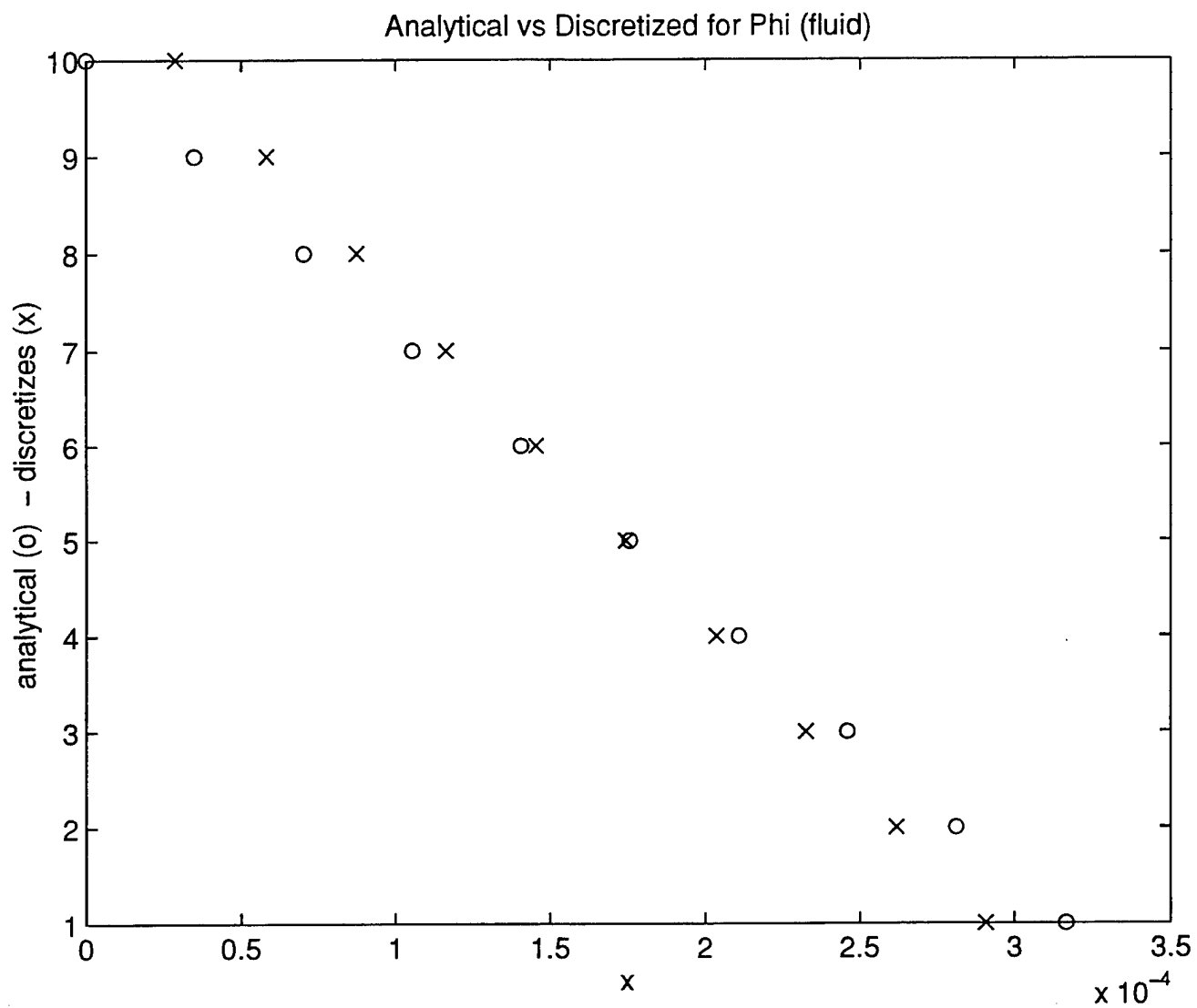


Figure 9. Analytical versus Discretized Solutions for ϕ

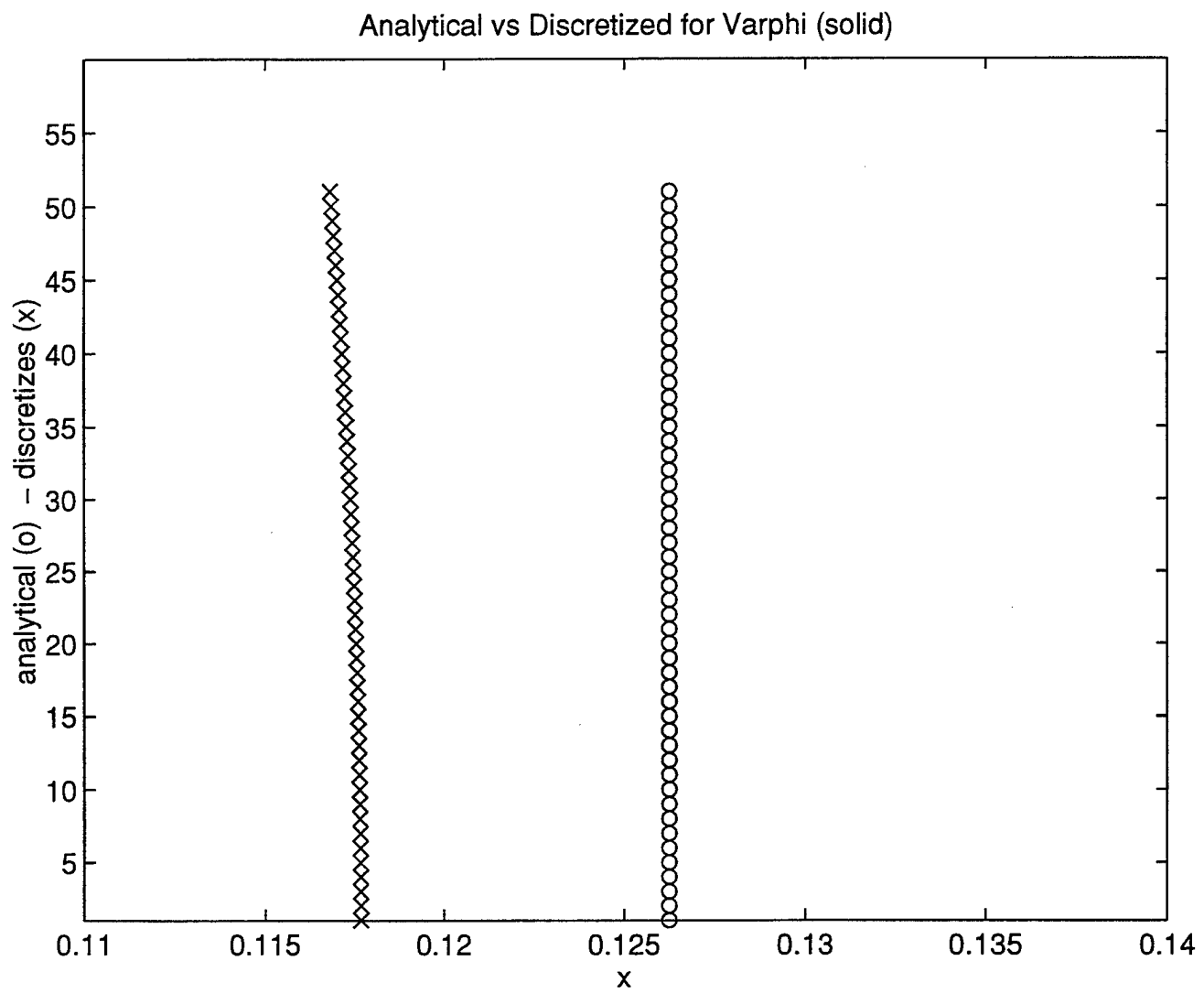


Figure 10. Analytical versus Discretized Solutions for φ

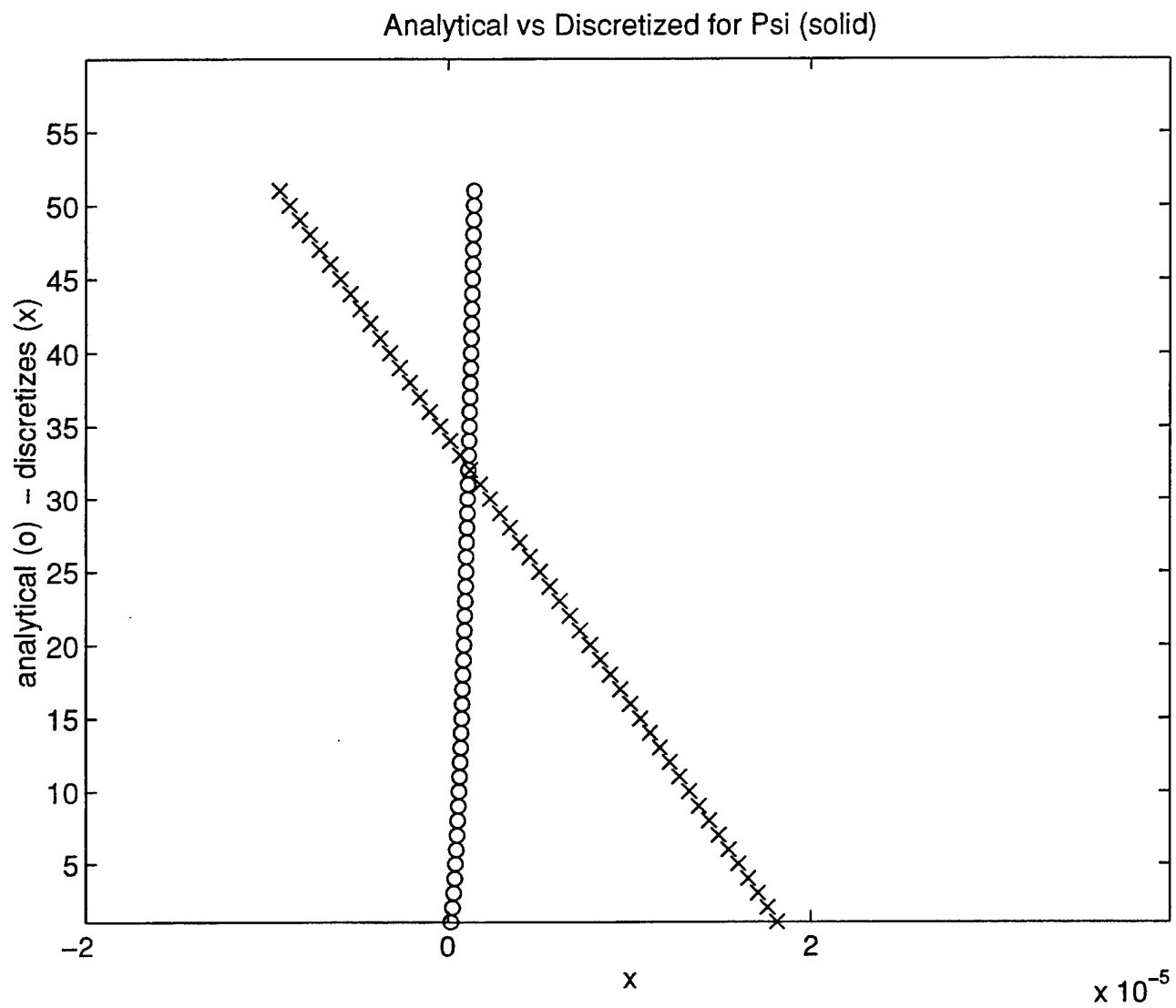


Figure 11. Analytical versus Discretized Solutions for ψ

Figure (12) illustrates a pressure-stress graph. Notice that at the boundary of the fluid and elastic layer a discontinuity exists. One of our boundary conditions from the fluid loaded plate is

$$\tau_{yy} = -p \quad (\text{IV.4})$$

This means that our plot should connect smoothly at the interface. The discontinuity indicates a problem with the discretization at the interface. This problem was evident in the previous plots and is re-enforced with this graph.

Figure (13) plots the wave numbers of the first three modes as a function of increasing frequency. We see that our fundamental mode is purely real and our second and third modes are complex.

3. Bi-orthogonality

The bi-orthogonality condition of differing modes from Chapter II indicates that we should expect a diagonal matrix in forming the bi-orthogonality product of a set of modes, where the diagonal element, x_n , is the “norm” of each individual mode.

$$x_n = \int_{-h_2}^0 [\tau_{xx}^{(n)} u^{(n)} - \tau_{xy}^{(n)} v^{(n)}]_{elastic} dy - \int_0^{h_1} [p^{(n)} U^{(n)}]_{fluid} dy \quad (\text{IV.5})$$

The bi-orthogonality condition states that the off-diagonal elements, the product of two separate modes, should go to zero. Numerically, we expect these elements to tend toward zero. The numerical bi-orthogonality relationship for the fluid loaded plate yields the following matrix:

$$\begin{bmatrix} 4.441 \times 10^5 & 4.561 \times 10^5 & 5.233 \times 10^3 & 3.639 \times 10^3 & 3.836 \times 10^3 \\ 4.561 \times 10^5 & 4.441 \times 10^5 & 5.233 \times 10^3 & 3.836 \times 10^3 & 3.639 \times 10^3 \\ 5.118 \times 10^5 & 5.118 \times 10^5 & 7.046 \times 10^5 & 2.670 \times 10^6 & 2.670 \times 10^6 \\ 2.617 \times 10^6 & 1.005 \times 10^7 & 6.139 \times 10^6 & 1.524 \times 10^7 & 1.832 \times 10^7 \\ 1.005 \times 10^7 & 2.617 \times 10^6 & 6.139 \times 10^6 & 1.832 \times 10^7 & 1.524 \times 10^7 \end{bmatrix} \quad (\text{IV.6})$$

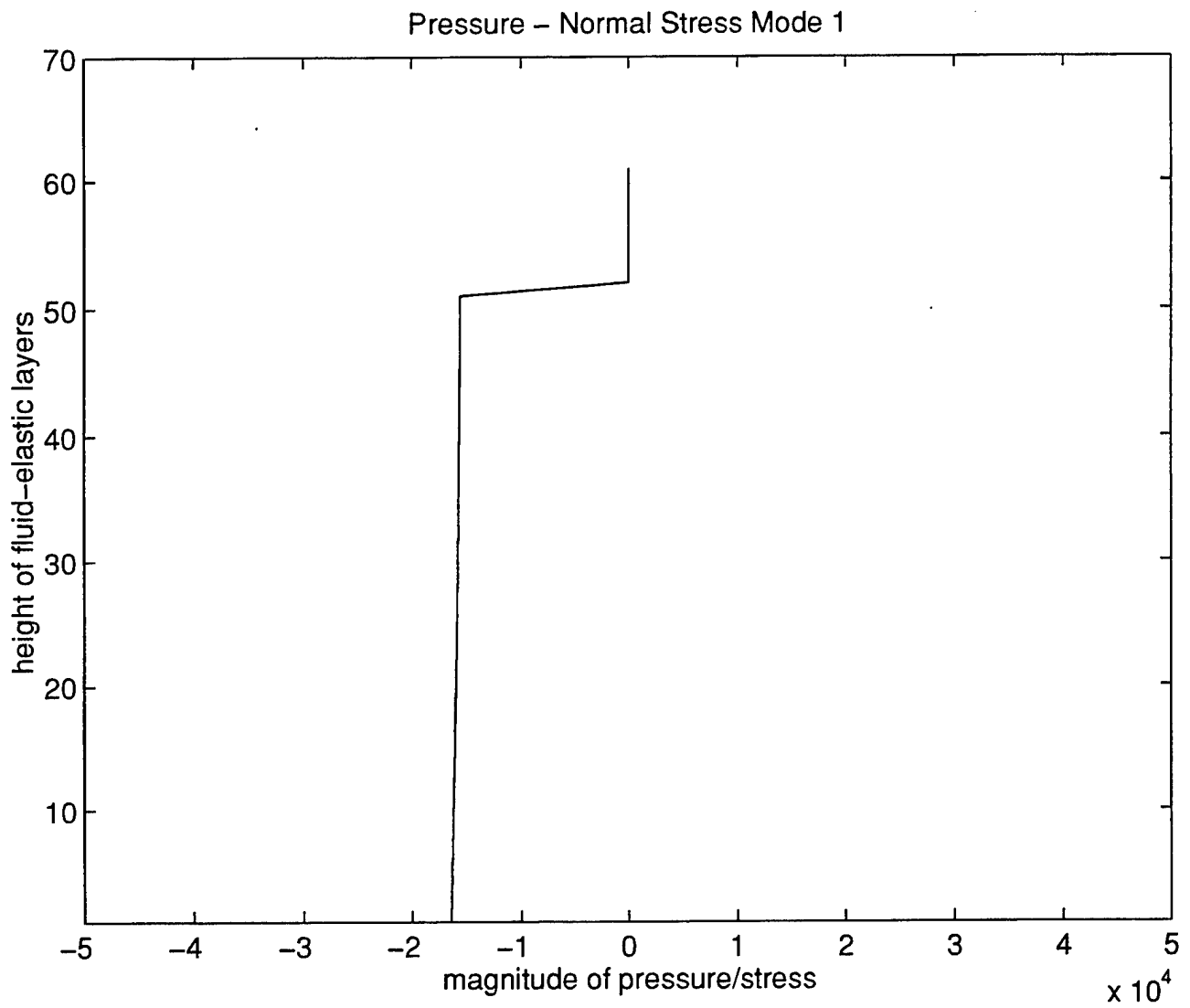


Figure 12. Pressure - Normal Stress in Layer

Wave Propagation for Steel

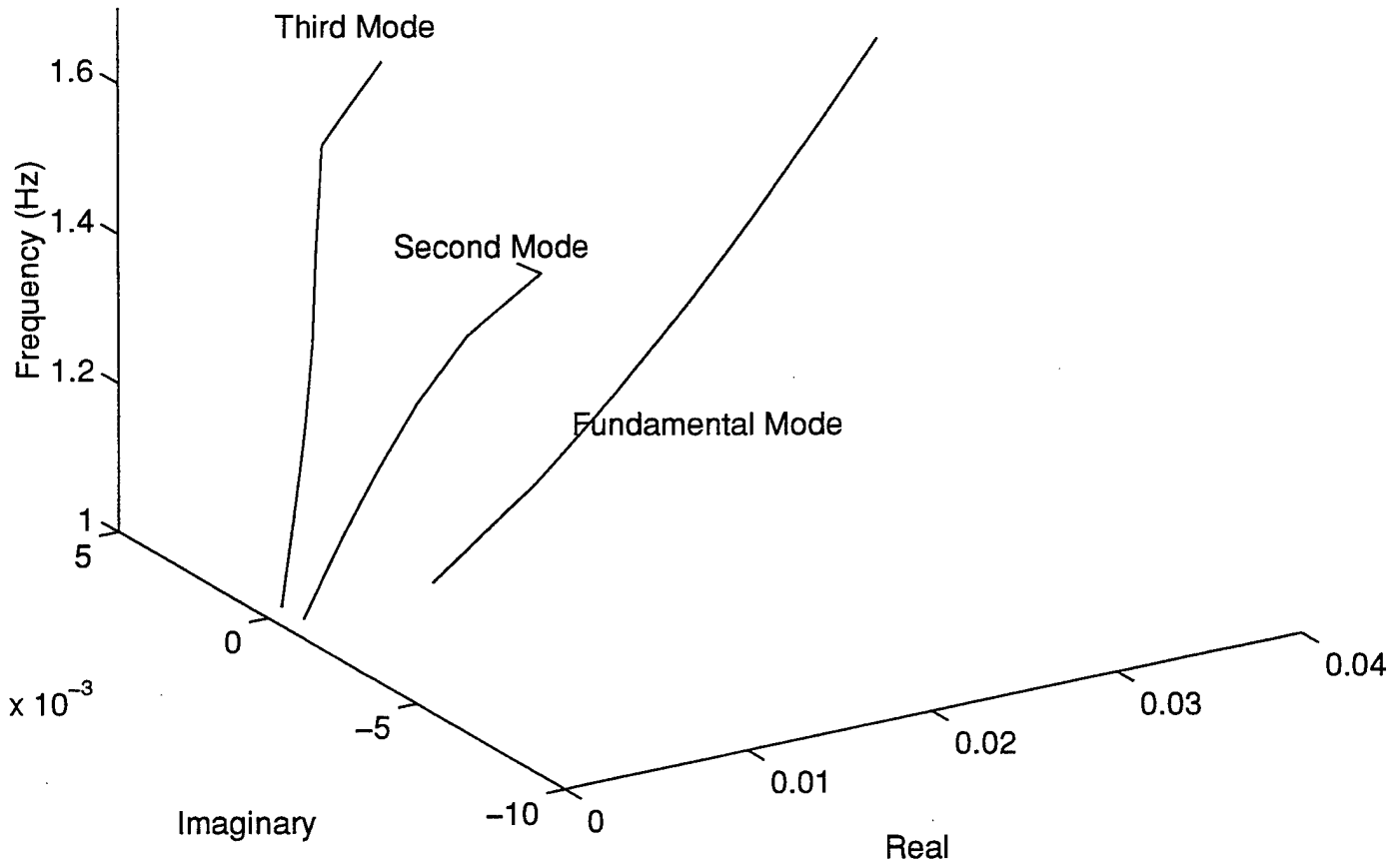


Figure 13. Wave Mode Propagation - Modes 1-3

Notice in this matrix, most of the off-diagonal elements tend to exhibit some form of reduction. However, this did not happen as quickly as believed. This indicates that the bi-orthogonality condition is very sensitive to small errors in calculating the modes. A more careful numerical treatment might improve the diagonal form of the matrix, but it may be necessary to limit the application of the numerical method to eigenmode determination only, from which the eigenmodes can be refined and ultimately found by analytical means.

V. CONCLUSIONS AND FUTURE RESEARCH

We can draw several conclusions on the discretization of the fluid loaded elastic plate. The eigenvalues, or modal wave numbers, that resulted from the discretization nearly satisfy the Dispersion Equation (III.39). Using Newton's Method, we determined that our initial values may not be close enough in some instances to the actual roots as is evidenced from the lack of improvement of the residual calculation in the "refined" root. Therefore, we conclude that there are numerous other roots that we have not found.

The biggest disparity lies in the plot of pressure and normal stress versus the height of the fluid and elastic layer. As seen in the discretization code in the Appendix, differencing of the potentials is necessary when solving for the stresses and displacements. Therefore, any numerical error in the fluid-elastic boundary differencing is compounded. Recall, in theory the normal stress is equal to minus the pressure at this boundary. The discretization does not show this. Finally, we conclude that our graph of the first three modes in Figure (13), could indeed be modes for this problem. However, they are most likely not the first three propagating modes.

The trouble with the results is mostly due to the following: a) there are errors in the discretization or b) the discretization is unable to properly model the boundary conditions. Indications of the first problem are evidenced in two ways. The first is the inability of the eigenvalues to converge to the correct analytical eigenvalues. Secondly, the plotting of the corresponding eigenvectors do not satisfy the boundary conditions as required. The solution to this problem is to find the correct way to difference the boundary conditions. Nothing can be done to fix the second problem, except to try a different discretization. The code as it stands does find some roots, but until the boundary conditions can be satisfied, there is no real confidence that the roots are comprehensive.

Several new problems arise from this research. The first is to determine a better way of differencing the boundary of the fluid-elastic layer. Once this problem is corrected, we can solve for the coefficients of transmitted and reflected waves given an incident wave. This is useful when extending the elastic case to the more complex porous case. If the porous case can be solved numerically, this will allow us to create ocean acoustic models where the transmitted and reflected waves can be determined from known coefficients. This has potential applications in sonar and mapping of the ocean floor. Finally, a similar problem involves modeling a fluid layer only, with different sound velocity profiles and an acoustically hard boundary. The discretization would not involve the elastic boundary and may be a better way to approach the fluid-elastic case.

APPENDIX. MISCELLANEOUS DATA

1. MATLAB CODE FOR GENERATING WAVE SPEEDS

```
function [] =elastic(E, nu, rho)

% *****
% ELASTIC - This function computes the elastic constants and
%           wavespeeds for various solids. Input values are the
%           Young's Modulus, Poisson's ratio, and the density.
%
% Copyright 1997 by C. R. Myers, III
% *****

lambda=0;
mu=0;
cl=0;
ct=0;
E=E*10^10;

lambda = (E*nu)/((1+nu)*(1-2*nu))
mu = E/(2*(1+nu))
cl = round(sqrt((lambda + 2*mu)/rho));
ct = round(sqrt(mu/rho));
```

2. DISCRETIZATION MATLAB CODE

```
% *****
% Fluid-Elastic Finite Difference Matlab Code
%
% Copyright 1998 by Coley R. Myers, III
% *****

% Initialize
clear;
format long e;
w=0;
E_val=[];

% allows program to run in loop for obtaining
% modes over a specified frequency range.
```

```

counter=1;

% loop is a counter and is used to obtain graph
% graph of modes over a specified frequency range

for loop=1:counter

% Variables input for specific elastic solids
% *****

I=sqrt(-1);
Lf=10;
Ls=200;
w=2*pi+(w+.1); rf=1026; rs=7700;
ct=3145; cl=5690; cf=1500;
modes=10;
mu=rs*ct^2;
lam=rs*cl^2 - 2*mu;
hf=1;
hs=4;
N=Lf/hf;
M=Ls/hs;
d=N+M+M+2;
A=zeros(d);
kf=w/cf; kt=w/ct; kl=w/cl;

% Ensures matrices are clear when loop > 1

V1=[];Phi=[];Vphi=[];Psi=[];Psixy=[];Vphiy=[];
V=[];D=[];Pres=[];U=[];
u=[];v=[];Styy=[];Stxx=[];Stxy=[];
pr_styy=[];f1=[];F1=[];Y=[];Y1=[];
Vphia=[];Psia=[];Phia=[];

% Fluid BC Phi(0)=0 and 1st equation

p=1;
A(p,1)=-(2/hf^2-kf^2);
A(p,2)=1/hf^2;
p=p+1;

for i=2:N-1

```

```

    A(p,i-1)=1/hf^2;
    A(p,i)=-(2/hf^2-kf^2);
    A(p,i+1)=1/hf^2;
    p=p+1;

end;

% 3rd BC for Phi

A(p,N-1)=2/hf^2;
A(p,N)=-2/hf^2+kf^2+(hs*w^2*rf)/(mu*hf);
A(p,N+1)=(w^2/(hs*hf))*(1+hs^2*(kt^2-kl^2));
A(p,N+2)=-hs*w^2*kl^2/hf;
A(p,N+3)=-w^2/(hs*hf);
A(p,N+M+2)=(kt^2*hs^2*w^2)/(2*hf);
A(p,N+M+3)=-2*w^2/hf;

% 1st BC for Varphi

p=p+1;
A(p,N+M+2)=(2/hs)+kt^2*hs/2;
A(p,N+M+3)=-2/hs;
A(p,N+3)=-1/hs^2;
A(p,N+2)=(2/hs^2)-kl^2;
A(p,N+1)=kt^2-1/hs^2;
A(p,N)=rf/mu;
p=p+1;

% 2nd BC for Varphi

for i=(N+2):(N+M)

    A(p,i-1)=1/hs^2;
    A(p,i)=-(2/hs^2-kl^2);
    A(p,i+1)=1/hs^2;
    p=p+1;

end;

% 3rd BC for Varphi

```

```

A(p,N+2*M+2)=(kt^2*hs/2)-2/hs;
A(p,N+2*M+1)=2/hs;
A(p,N+M+1)=kt^2-1/hs^2;
A(p,N+M)=2/hs^2-kl^2;
A(p,N+M-1)=-1/hs^2;
p=p+1;

```

```

% 1st BC for Psi

```

```

A(p,N)=rf/(mu*hs);
A(p,N+1)=kt^2/hs-2/hs^3;
A(p,N+2)=4/hs^3-2*kl^2/hs;
A(p,N+3)=-2/hs^3;
A(p,N+M+2)=2/hs^2;
A(p,N+M+3)=-2/hs^2;
p=p+1;

```

```

% 2nd BC for Psi

```

```

for i=(N+M+3):(N+2*M+1)

```

```

    A(p,i-1)=1/hs^2;
    A(p,i)=-(2/hs^2-kt^2);
    A(p,i+1)=1/hs^2;
    p=p+1;

```

```

end;

```

```

% 3rd BC for Psi

```

```

A(p,N+M-1)=2/hs^3;
A(p,N+M)=(2*kl^2/hs)-4/hs^3;
A(p,N+M+1)=(2/hs^3)-kt^2/hs;
A(p,N+2*M+1)=-2/hs^2;
A(p,N+2*M+2)=2/hs^2;

```

```

% Final matrix is calculated

```

```

[V, D]=eig(A);
D=sqrt(diag(D));
[Y I1]=sort(D);

```

```

% Lambda holds the number of modes specified for
% use with later calculations

Lambda=Y(1:modes);

% when loop > 1, E_val holds values for graph
% of modes over a specified frequency range

E_val = [E_val Lambda];

% Orders eigenvectors

for i = 1:modes
    j=I1(i);
    V1=[V1 V(:,j)];
end

% Separates stress potentials for calculations

for i = 1:modes
    Phi = [Phi V1(1:N,i)];
    Vphi = [Vphi V1(N+1:N+M+1,i)];
    Psi = [Psi V1(N+M+2:d,i)];
end;

% *****
% Solve for Pressure

Pres = -rf.*Phi;
U = -(1/(I*w)).*Phi;

% *****
% Differencing for discretized potentials

eta2 = Lambda.^2 - kl^2;
xi2 = Lambda.^2 - kt^2;
zeta2 = Lambda.^2 - kf^2;

% Finding Psi_xy (same as Psi_yx)

j=1;
for i=1:modes

```

```

        Psixy(j,i)=-((Psi(j+1,i)- (1 + (hs^2/2).*xi2(i)).*Psi(j,i))./(
        (hs + (hs^3/6).*xi2(i))));
    end

    for j=2:M
        for i=1:modes
            Psixy(j,i)=(Psi(j-1,i)-Psi(j+1,i))/(2*hs);
        end
    end

    j=M+1;
    for i=1:modes
        Psixy(j,i)=(Psi(j-1,i)- (1 + (hs^2/2).*xi2(i)).*Psi(j,i))./(
        (hs + (hs^3/6).*xi2(i))));
    end

    % Finding Vphi_y

    j=1;
    for i=1:modes
        Vphiy(j,i)=-((Vphi(j+1,i)- (1 + (hs^2/2).*eta2(i)).*
        Vphi(j,i))./(hs + (hs^3/6).*eta2(i))));
    end

    for j=2:M
        for i=1:modes
            Vphiy(j,i)=(Vphi(j-1,i)-Vphi(j+1,i))/(2*hs);
        end
    end

    j=M+1;
    for i=1:modes
        Vphiy(j,i)=(Vphi(j-1,i)- (1 + (hs^2/2).*eta2(i)).*
        Vphi(j,i))./(hs + (hs^3/6).*eta2(i))));
    end

    % *****
    % Solving for Tau_yy, Tau_xy, and Tau_yy

    for i=1:modes

        Styy = [Styy (-((lam + 2*mu)*kl^2).*Vphi(:,i) - (2*mu).*

```

```

        Psixy(:,i))];
Stxx = [Stxx ((2*mu).*Psixy(:,i) - ((2*mu)*Lambda(i)^2 +
        lam*kl^2).*Vphi(:,i))];
Stxy = [Stxy (((2*mu*I)*Lambda(i).*Vphiy(:,i)) +
        (2*Lambda(i)^2 - kt^2)*(1/(I*Lambda(i))).*Psi(:,i))];

end;

% Solving for u and v

for i=1:modes
    u = [u (I.*Lambda(i).*Vphi(:,i)+(1/(I.*Lambda(i))).*
        Psixy(:,i))];
    v = [v (Vphiy(:,i) - Psi(:,i))];
end

% *****
% Applying bi-orthogonality condition

for i = 1:modes
    F1 = [Pres(:,i); Styy(:,i)];
    pr_styy = [pr_styy F1];
end

f1 = (Stxx'*u - Stxy'*v) - Pres'*U;

for j=1:modes
    for i=1:modes
        f1(i,j)=f1(i,j)*conj(f1(i,j));
    end
end

% *****
% Plot of norm of eigenvalues

Y1=sqrt(Y.*conj(Y));
i=56:-1:1;
figure
plot(Y1(1:56),i,'o')
title('Norm of Eigenvalues ')
xlabel('magnitude of lambda')
ylabel('modes')

```

```

% *****
% Determine coefficients for analytical solutions

k=Lambda(1,1);
deta2 = k^2 - kl^2;
dxi2 = k^2 - kt^2;
dzeta2 = k^2 - kf^2;
hs=200;
hf=10;
h=hf+hs;
% Change value for C
C=.00004;
D1=(2*k^2-kt^2)^2*tanh(sqrt(deta2)*(hs/2));
D2=4*k^2*sqrt(deta2)*sqrt(dxi2)*tanh(sqrt(dxi2)*(hs/2));
D3=(2*k^2-kt^2)^2*coth(sqrt(deta2)*(hs/2))*tanh(sqrt(dxi2)*
(hs/2));
D=(D1-D2)/(D3-4*k^2*sqrt(deta2)*sqrt(dxi2));
B1=-(2*k^2-kt^2)/(2*I*k*sqrt(deta2));
B2=(cosh(sqrt(dxi2)*(hs/2))/cosh(sqrt(deta2)*(hs/2)))*C;
B=B1*B2;
A2=(sinh(sqrt(dxi2)*(hs/2))/sinh(sqrt(deta2)*(hs/2)))*D;
A=B1*A2;
E1=(D1-D2)*C;
E2=ct/(k*kt*sqrt(deta2)*(rf/rs));
E3=cosh(sqrt(dxi2)*hs/2)/sinh(sqrt(dzeta2)*(hf+hs/2));
E=E1*E2*E3;

y=101:-1:1';
y1=M+1:-1:1;
y2=N:-1:1;

Vphia = A.*cosh(sqrt(deta2.*y1)) + B.*sinh(sqrt(deta2.*y1));
Psia = C.*cosh(sqrt(dxi2.*y1)) + D.*sinh(sqrt(dxi2.*y1));
Phia = E.*sinh(sqrt(dzeta2).*(N-y2));

% *****
% Plot analytical vs discretized solutions

figure
Vphia=sqrt(Vphia.*conj(Vphia));
plot(Vphia,y1,'o',Vphi(:,1),y1,'x')

```

```

title('Analytical vs Discretized for Varphi (solid)')
xlabel('x')
ylabel('analytical (o) - discretizes (x)')

```

```

figure
Psia = Psia.*I.*k;
Psia = sqrt(Psia.*conj(Psia));
plot(Psia,y1,'o',Psi(:,1),y1,'x')
title('Analytical vs Discretized for Psi (solid)')
xlabel('x')
ylabel('analytical (o) - discretizes (x)')

```

```

figure
Phia = I.*w.*Phia;
Phia = sqrt(Phia.*conj(Phia));
plot(Phia,y2,'o',Phi(:,1),y2,'x')
title('Analytical vs Discretized for Phi (fluid)')
xlabel('x')
ylabel('analytical (o) - discretizes (x)')

```

```

% *****

```

```

% end loop

```

```

end

```


LIST OF REFERENCES

- [1] C. L. Scandrett and C. L. Frenzen. Bi-orthogonality relationships involving porous media. *Journal of the Acoustical Society of America*, 98(2):1199–1203, August 1995.
- [2] W. B. Fraser. Orthogonality relation for the Rayleigh-Lamb modes of vibration of a plate. *Journal of the Acoustical Society of America*, 59(1):215–216, January 1976.
- [3] Clyde Scandrett and Naresh Vasudevan. The propagation of time harmonic Rayleigh-Lamb waves in a bimaterial plate. *Journal of the Acoustical Society of America*, 89(4):1606–1614, April 1991.
- [4] Curtis F. Gerald and Patrick O. Wheatley. *Applied Numerical Analysis 5th Edition*. Addison-Wesley, New York, 1994.
- [5] The MathWorks, Inc. *MATLAB High-Performance Numeric Computation and Visualization Software Reference Guide*. The MathWorks, Natick, Massachusetts, 1982.
- [6] Lawrence E. Kinsler and Austin R. Frey. *Fundamentals of Acoustics 3rd ed.* John Wiley and Sons, New York, New York, 1982.
- [7] J. D. Achenbach. *Wave Propagation in Elastic Solids*. North-Holland, The Netherlands, 1973.
- [8] Richard Haberman. *Elementary Applied Partial Differential Equations*. Prentice-Hall, Englewood Cliffs, New Jersey, 1983.

INITIAL DISTRIBUTION LIST

1. Defense Technical Information Center 2
8725 John J. Kingman Road., Ste 0944
Ft. Belvoir, VA 22060-6218
2. Dudley Knox Library 2
Naval Postgraduate School
411 Dyer Rd.
Monterey, CA 93943-5101
3. Chairman, Code MA 1
Department of Mathematics
Naval Postgraduate School
1411 Cunningham Road, Rm 341
Monterey, CA 93943-5216
4. Professor Clyde L. Scandrett, Code MA/Sc 2
Department of Mathematics
Naval Postgraduate School
1411 Cunningham Road, Rm 341
Monterey, CA 93943-5216
5. Professor Chris Frenzen, Code MA/Fr..... 2
Department of Mathematics
Naval Postgraduate School
1411 Cunningham Road, Rm 341
Monterey, CA 93943-5216
6. Lieutenant Coley R. Myers, III..... 5
267 Sunset Drive
Lexington, NC 27292